ChemPubSoc Europe

DOI: 10.1002/chem.201900732

CHEMISTRY A European Journal Full Paper

Nucleotides

Proton Transfer Accompanied by the Oxidation of Adenosine

Jungkweon Choi[+],[a, b] Sachiko Tojo[+],[c] Doo-Sik Ahn,[a, b] Mamoru Fujitsuka,*[c] Shunichi Miyamoto,[c] Kazuo Kobayashi,[c] Hyotcherl Ihee,*[a, b] and Tetsuro Majima*[c]

Abstract: Despite numerous experimental and theoretical studies, the proton transfer accompanying the oxidation of 2′-deoxyadenosine 5′-monophosphate 2′-deoxyadenosine 5′-monophosphate (5′-dAMP, **A**) is still under debate. To address this issue, we have investigated the oxidation of **A** in acidic and neutral solutions by using transient absorption (TA) and time-resolved resonance Raman (TR^3) spectroscopic methods in combination with pulse radiolysis. The steady-state Raman signal of **A** was significantly affected by the solution pH, but not by the concentration of adenosine (2–50 mM). More specifically, the **A** in acidic and neutral solutions exists in its protonated ($\mathbf{A}H^+(N1+H^+)$) and neutral (**A**) forms, respectively. On the one hand, the TA spectral changes observed at neutral pH revealed that the radical cation ($\mathbf{A}^{\bullet+}$) generated by pulse radiolysis is rapidly converted into $\mathbf{A}^{\bullet}(N6-H)$ through the loss of an imino proton from N6. In contrast, at acidic pH (<4), $\mathbf{A}H^{\bullet 2+}(N1+H^+)$ generated by pulse radiolysis of $\mathbf{A}H^+(N1+H^+)$ does not undergo the deprotonation process owing to the pK_a value of $\mathbf{A}H^{\bullet 2+}(N1+H^+)$, which is higher than the solution pH. Furthermore, the results presented in this study have demonstrated that **A**, $\mathbf{A}H^+(N1+H^+)$, and their radical species exist as monomers in the concentration range of 2–50 mM. Compared with the Raman bands of $\mathbf{A}H^+(N1+H^+)$, the TR^3 bands of $\mathbf{A}H^{\bullet 2+}(N1+H^+)$ are significantly down-shifted, indicating a decrease in the bond order of the pyrimidine and imidazole rings due to the resonance structure of $\mathbf{A}H^{\bullet 2+}(N1+H^+)$. Meanwhile, $\mathbf{A}^{\bullet}(N6-H)$ does not show a Raman band corresponding to the pyrimidine $+NH_2$ scissoring vibration due to diprotonation at the N6 position. These results support the final products generated by the oxidation of adenosine in acidic and neutral solutions being $\mathbf{A}H^{\bullet 2+}(N1+H^+)$ and $\mathbf{A}^{\bullet}(N6-H)$, respectively.

Introduction

The oxidation and reduction of DNA are central to the DNA damage and repair processes. For example, in a biological system, oxidative DNA damage is initiated by the radical cations of nucleotides generated during the oxidation of DNA. In this regard, the radical species generated during the oxidation and reduction of the four nucleobases (**A**, **T**, **G**, and **C**) have received considerable attention in the biochemical and biomedical sciences. Considering the redox potentials of the four nucleobases (**A**, **T**, **G**, and **C**),[1] **T** and **C,** with the highest oxidation potentials, are relatively easily reduced to the radical anions $\mathbf{T}^{\bullet-}$ and $\mathbf{C}^{\bullet-}$, whereas **G** and **A,** with lower oxidation potentials, are easily oxidized to the radical cations $\mathbf{G}^{\bullet+}$ and $\mathbf{A}^{\bullet+}$.[1–9] In addition, the oxidation and reduction of DNA includes a proton-transfer process. For example, monomeric $\mathbf{G}^{\bullet+}$ in aqueous solution quickly converts into the neutral radical ($G^{\bullet}(N1-H)$) through the loss of the imino proton at N1 (deprotonation).[7,10,11] In double-stranded DNA, proton transfer takes place in the $\mathbf{G}^{\bullet+}$-**C** base pair from N1 of $\mathbf{G}^{\bullet+}$ to N3 of **C**; $\mathbf{G}^{\bullet+}$-**C** $\rightarrow \mathbf{G}^{\bullet}(N1-H)$-$\mathbf{C}^+(N3+H^+)$.[6,9,12] Moreover, Wu et al. reported an unusual deprotonation behavior, namely the loss of an amino proton from N2 instead of the imino proton at N1 of $\mathbf{G}^{\bullet+}$ within the **G** quadruplex.[8] Recently we demonstrated that reprotonation at the N7 position of $\mathbf{G}^{\bullet}(N1-H)$, which is formed by the deprotonation of $\mathbf{G}^{\bullet+}$, occurs with a rate constant of $8.1\times10^6\ s^{-1}$ in 100 mM sodium phosphate buffer (pH 7.4): $\mathbf{G}^{\bullet}(N1-H)+H^+\rightarrow(\mathbf{G}^{\bullet+})'$.[13] This reprotonation process at the N7 position of $\mathbf{G}^{\bullet}(N1-H)$ was independently confirmed by Morozova et al.[14]

Despite numerous experimental and theoretical studies, however, there is still no consensus on the dynamics of proton transfer nor on the structures and reactivities of the radical species of the four nucleobases. In particular, the dynamics of proton transfer accompanying the oxidation of 2′-deoxyadeno-

[a] Dr. J. Choi,[+] Dr. D.-S. Ahn, Prof. Dr. H. Ihee
Center for Nanomaterials and Chemical Reactions
Institute for Basic Science (IBS), Daejeon 305-701 (Republic of Korea)
E-mail: hyotcherl.ihee@kaist.ac.kr

[b] Dr. J. Choi,[+] Dr. D.-S. Ahn, Prof. Dr. H. Ihee
Department of Chemistry and KI for the BioCentury
Korea Advanced Institute of Science and Technology (KAIST)
Daejeon 305-701 (Republic of Korea)

[c] S. Tojo,[+] Prof. Dr. M. Fujitsuka, S. Miyamoto, Prof. Dr. K. Kobayashi, Prof. Dr. T. Majima
The Institute of Scientific and Industrial Research (SANKEN)
Osaka University, Mihogaoka 8-1, Ibaraki, Osaka 567-0047 (Japan)
E-mail: fuji@sanken.osaka-u.ac.jp
majima@sanken.osaka-u.ac.jp

[+] These authors contributed equally to this work.

Supporting information and the ORCID identification number(s) for the author(s) of this article can be found under: https://doi.org/10.1002/chem.201900732.

sine 5′-monophosphate (5′-dAMP, **A**) has been debated. Furthermore, the formation of dimeric $\mathbf{AA}^{\bullet+}$ and its pK_a are also under debate. Generally, the dynamics of proton transfer are greatly influenced by the pK_a values of the nucleobases as well as by the pH of the solution. In this regard, it is critical to accurately determine the pK_a values of adenosine and its radical species. The pK_a of **A** has been experimentally and theoretically determined to be approximately 4,[15,16] which indicates that adenosine exists in its protonated ($\mathbf{AH}^+$) and neutral (**A**) forms in acidic and neutral pH solutions, respectively. Thus, the oxidation of $\mathbf{AH}^+$ in acidic pH solutions should be significantly different to that of **A** in neutral pH solutions and should induce the generation of different radical species, namely $\mathbf{AH}^{\bullet 2+}$ and $\mathbf{A}^{\bullet+}$, respectively (see Scheme 1). However, the results of several studies have suggested that **A** even in acidic pH solution exists as the neutral form **A**, not $\mathbf{AH}^+$.[7,11,17] Consequently, these results suggested that **A** in acidic solution is converted into $\mathbf{A}^{\bullet+}$ by one-electron oxidation and can further transform into $\mathbf{A}^{\bullet}$(N6−H) by subsequent deprotonation.[7,11,17] Moreover, the results of some studies have suggested that free **A** bases, such as 5′-dAMP and 2′-deoxyadenosine monohydrate, associate to yield the stacked form (**AA**) in high-concentration solutions (>10 mM) with the one-electron oxidation of **AA** resulting in the formation of a dimer radical cation ($\mathbf{AA}^{\bullet+}$) stabilized by charge resonance.[7,17] Sevilla and co-workers suggested that the pK_a of $\mathbf{A}^{\bullet+}$ isolated in solution is vastly different to that of $\mathbf{A}^{\bullet+}$ in $\mathbf{AA}^{\bullet+}$: The pK_a values are less than 1 for monomeric $\mathbf{A}^{\bullet+}$ and approximately 7 for $\mathbf{AA}^{\bullet+}$.[17]

In this work, to directly monitor the dynamics of proton transfer in adenosine radical species, we investigated in detail the oxidation of free **A** in both acidic and neutral pH solutions by using transient absorption (TA) and time-resolved resonance Raman (TR^3) spectroscopic methods in combination with pulse radiolysis. Pulse radiolysis, which has been long used as a useful method to selectively and efficiently generate radical ions by irradiation with high-energy electrons, is a novel tool for investigating intermediate species such as radicals and radical ions when used in combination with other spectroscopic techniques. Indeed, transient absorption (TA) spectroscopy in combination with pulse radiolysis is a useful method for studying the reactivities of radical ions generated in various reaction systems.[13,18–20] Furthermore, TR^3 spectroscopy in combination with pulse radiolysis is a powerful technique for studying the structures of radical species involved in a reaction system.[13,21,22] The results presented herein reveal that **A** exists in its protonated ($\mathbf{AH}^+$(N1 + H^+)) and neutral (**A**) forms in acidic (pH < 4) and neutral pH (pH > 5) solutions, respectively. At neutral pH, $\mathbf{A}^{\bullet+}$, formed by the one-electron oxidation of **A**, is rapidly converted into the radical $\mathbf{A}^{\bullet}$(N6−H) through the loss of an imino proton from N6 (deprotonation). However, at acidic pH (≤4), $\mathbf{AH}^{\bullet 2+}$(N1 + H^+), generated with a rate constant of $(6.2\pm0.5)\times10^6\ s^{-1}$ by the pulse radiolysis of $\mathbf{AH}^+$(N1 + H^+), does not undergo the deprotonation process because its pK_a is higher than the pH of the solution. Moreover, the data show that **A**, $\mathbf{AH}^+$(N1 + H^+), and their radical species exist as monomers in the concentration range of 2–50 mM. We note that the TR^3 spectra of $\mathbf{AH}^{\bullet 2+}$(N1 + H^+) and $\mathbf{A}^{\bullet}$ generated during the pulse radiolysis of $\mathbf{AH}^+$(N1 + H^+) and **A**, respectively, are reported for the first time and are interpreted in terms of the structural changes accompanying the proton dynamics.

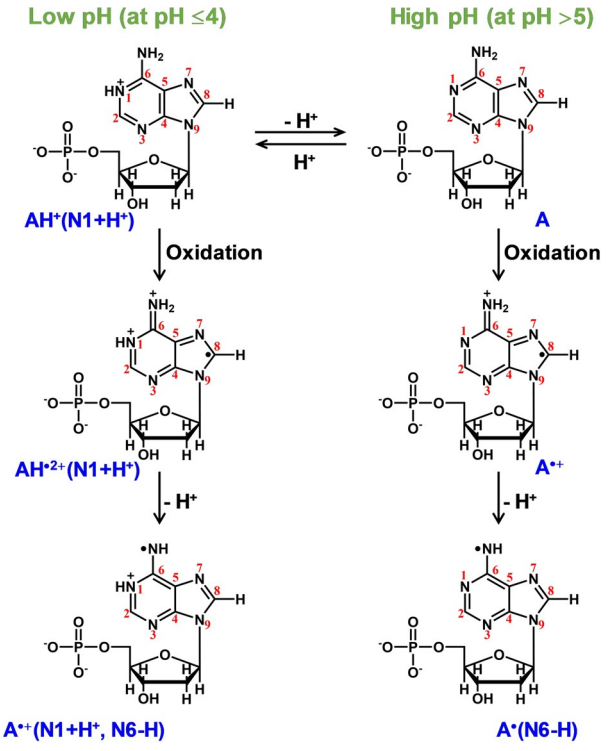

Scheme 1. Oxidation and deprotonation of adenosine in acidic and neutral pH solutions.

Results and Discussion

According to the previous reports that the pK_a of **A** is approximately 4,[7,15,16] **A** exists as $\mathbf{AH}^+$ in acidic solutions (which in this work is defined as solutions with pH < 4). Therefore, the oxidation of $\mathbf{AH}^+$ in acidic solutions by pulse radiolysis should induce the generation of radical species such as $\mathbf{AH}^{\bullet 2+}$ and $\mathbf{A}^{\bullet+}$ (see Scheme 1). In acidic solutions, protons can bind to the N1, C2, N3, N6, N7, and C8 positions of adenosine. Based on the results of their ab initio and DFT calculations, Tureček and Chen suggested that N1-protonated adenosine, $\mathbf{AH}^+$(N1 + H^+), is the most stable cationic tautomer in the gas phase, water clusters, and bulk solution.[23] Therefore, we first investigated whether in acidic solutions **A** exists preferentially in the N1-protonated form $\mathbf{AH}^+$(N1 + H^+).

To verify the existence of $\mathbf{AH}^+$(N1 + H^+) in acidic solutions, we measured the steady-state Raman spectrum of **A** in acidic solution and compared it with that measured in neutral solution. As shown in Figure 1a, the Raman spectrum of **A** measured in acidic solution (pH 2.6) is very different to that measured in neutral solution (pH 7.0). The differences in the Raman spectra are probably due to the protonation of the purine moiety ($pK_a \approx 4$), and thus we attribute the Raman spectra measured at pH 2.6 and 7.0 to $\mathbf{AH}^+$ and **A**, respectively. As depicted in Figure 1a, the steady-state Raman spectrum of **A** shows intense bands centered at 1308, 1339, 1377, 1421, 1481,

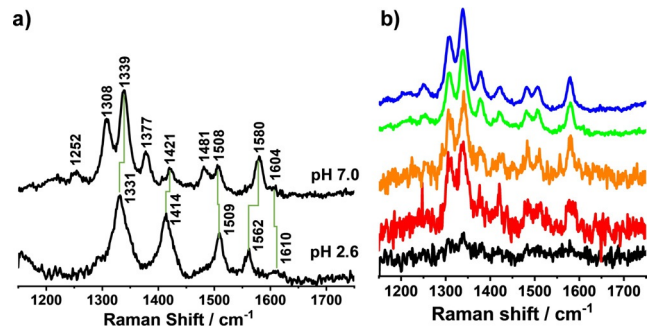

Figure 1. a) Steady-state Raman spectra of 20 mM AH^+ and 20 mM **A** at pH 2.6 and 7.0. b) Concentration dependence of the steady-state Raman spectra of **A** at pH 7.0 (from bottom to top: 2 (black), 4 (red), 10 (orange), 20 (green), and 50 mM **A** (blue)).

1508, and 1580 cm^{-1}, whereas the steady-state Raman spectrum of AH^+ shows intense Raman bands centered at 1331, 1414, 1509, and 1562 cm^{-1}. The Raman spectra of AH^+ and **A** recorded in this study are consistent with those reported by Lord and Thomas.[24] In addition, the calculated Raman activities of $AH^+(N1+H^+)$ and **A** agree well with those of AH^+ and **A** measured in the present study (see Figure S1 in the Supporting Information), which supports the idea that the proton binds to the N1 position of **A** in acidic solution to form $AH^+(N1+H^+)$. The Raman bands of **A** at neutral pH have been assigned (Table 1) on the basis of the results of the calculations and the assignments of the Raman spectra of 5′-dAMP reported previously by Bailey et al.,[25] Lord and Thomas,[24] Fodor and Spiro,[26] Fujimoto et al.,[27] and Toyama et al.[28] The two strong bands at 1308 and 1339 cm^{-1} correspond to pyrimidine (Pyr) ring stretching vibrations, and the bands at 1377, 1421, 1481, 1508, and 1580 cm^{-1} have been assigned to pyrimidine (Pyr) + imidazole (Im), Im, Pyr + Im, Im, and Pyr ring stretching vibrations, respectively. The weak Raman band at 1604 cm^{-1} has been attributed to the Pyr + NH_2 scissoring vibration. Based on the intense calculated Raman activities of $AH^+(N1+H^+)$ (see Figure S1 in the Supporting Information), the Raman bands centered at 1331, 1414, 1509, and 1562 cm^{-1} have been assigned to Pyr(N7C5 + C8N7), Im, Im, and Pyr ring stretching vibrations, respectively. The weak Raman band at 1610 cm^{-1} has been attributed to the Pyr + NH_2 scissoring vibration. As shown in Table 1, the Raman bands (1610 and 1509 cm^{-1}) of $AH^+(N1+H^+)$, with a high contribution from the δHN6H′−δC6N6H′ stretching mode, are slightly shifted to a higher energy relative to those of the neutral form **A**, whereas protonation results in a shift to a lower energy of the Pyr ring stretching mode (1560, 1414, and 1331 cm^{-1}).

It has been suggested that at neutral pH, the free **A** base (5′-dAMP or 2′-deoxyadenosine monohydrate) exists in the stacked form (**AA**) in high-concentration solutions (>10 mM).[7,17] In contrast, the dimerization of $AH^+(N1+H^+)$ at acidic pH is likely to remain limited due to coulombic repulsion between two positively charged $AH^+(N1+H^+)$. To characterize the structure of **A** in high-concentration solutions, we measured the steady-state Raman spectra of **A** as a function of concentration at pH 7.0 (Figure 1 b). As shown in Figure 1 b, the Raman spectrum of **A** measured at a low concentration (2 mM) is consistent with those measured at high concentrations (20 and 50 mM), which suggests that **A** exists predominantly as a monomer even in highly concentrated solutions. To confirm this, we calculated the minimum-energy structures of various **A** dimers (**AA**). Of these, we considered two representative adenosine dimers: Hydrogen-bonded and stacked **A** dimers. Their Raman activities were calculated and compared with the experimental and calculated Raman spectra of **A** (see Figure S2 in the Supporting Information). As shown in Figure S2, the calculated Raman spectra of the two **A** dimers are different to that of the **A** monomer. The hydrogen-bonded **A** dimer shows Raman bands at 1601 and 1653 cm^{-1}, which correspond to Pyr + NH_2 and NH_2 scissoring vibrations, respectively, whereas the calculated Raman spectra of the monomer and stacked **A** dimer show only a Raman band corresponding to the Pyr + NH_2 scissoring vibration. In contrast to the monomer and hydrogen-bonded **A** dimer, the stacked **A** dimer shows relatively broad Raman bands. As shown in Figure S2, the mea-

Table 1. Raman bands for AH^+, $AH^{\bullet 2+}$, **A**, and $A^\bullet$ observed in acidic and neutral solutions containing 0.1 M $(NH_4)_2S_2O_8$ and 0.1 M *tert*-butyl alcohol.

Assignment of Raman bands[a]	AH^+ at pH 2.6 [cm^{-1}][b]	$AH^{\bullet 2+}$ at pH 2.6 [cm^{-1}][b]	**A** at pH 7.0 [cm^{-1}][b]	$A^\bullet$ at pH 7.0 [cm^{-1}][b]
Pyr + NH_2 scissoring δHN6H′ (36)-δC6N6H′ (11)	1610 (1603)	1546	1604 (1611)	–
purine ring stretching	1562 (1554)	1462	1580 (1572)	1572
δC6N6H′ (16) + νN3C4 (13)–δHN6H′ (12)	1509(1503)	1394	1508 (1496)	1525
δHN6H′ (15)–τN3C4C5C6 (14) + τC2N3C4C5 (10) + ≈Im ring contributions (10)	–	–	1481 (1463)	1445
δN1C2H (12) + δN9C8H (10)–δN3C2H2 (8)–δC1′C2′H (7) + νC2N3 (7)–δN6C8H (4) + νC8N9 (4)	1414 (1419)	1377	1421 (1410)	1391
δHN6H′ (20)–δN9C8H (18) + δN7C8H (11)	–	–	1377 (1362)	1329
δC2′C1′H (18)–δHN6H′ (16) + δC6N6H (5) + δC6N6H′ (3)–δN3C2H (2) + νN9C1′ (2)–νC8N9 (2)	1331 (1347)	–	1339 (1340)	–
δN1C2H(39)–δN3C2H (16)–δN1C2N3 (6)–νN1C6 (3) + δHN6H′ (3) + δC6N1C2 (2) + νC5N7 (2)	–	–	1308 (1303)	–
δN3C2H (14)–δN1C2H (9)	–	–	1252 (1217)	1267

[a] ν = stretching; δ = in-plane bending. Percent contribution (in parentheses) from bond stretching or bending coordinates. [b] Values in parentheses are the calculated wavenumbers.

sured Raman spectrum of **A** shows the best agreement with the Raman spectrum calculated for **A** monomer, which suggests that **A** at neutral pH exists as a monomer even in high-concentration solutions. These results are in agreement with those reported by Neurohr and Mantsch,[29] who reported that the equilibrium constant (K_c) for the self-association of adenosine 5′-monophosphate is 1.92 M^{-1} at 30 °C. On the basis of this data, the amount of stacked **AA** formed in a 20 mM **A** solution would be very small (3.6%). Thus, we conclude that **A** predominantly exists as a monomer under our experimental conditions ($\leq$20 mM **A**).

To elucidate the dynamics of proton transfer accompanying the formation of $\mathbf{AH}^{\bullet 2+}$(N1 + H^+) and $\mathbf{A}^{\bullet +}$, we measured the TA spectra of the radical species at various times after pulse radiolysis of $\mathbf{AH}^+$(N1 + H^+) and **A** in solutions at pH 2.3 and 7.0, respectively. $\mathbf{AH}^{\bullet 2+}$(N1 + H^+) and $\mathbf{A}^{\bullet +}$ can be easily formed by the oxidation of $\mathbf{AH}^+$(N1 + H^+) and **A** using pulse radiolysis. At pH 7.0, the hydrated electron (e_{aq}^-) generated during pulse radiolysis in an aqueous solution containing $(NH_4)_2S_2O_8$ and *tert*-butyl alcohol (as scavenger of OH$^\bullet$ radicals) quickly reacts with the peroxydisulfate ($S_2O_8^{2-}$) to produce a sulfate radical anion ($SO_4^{\bullet -}$), which is a strong oxidant [Reaction (1)].[7,11,30–32] The $SO_4^{\bullet -}$ radical anion then oxidizes **A** to $\mathbf{A}^{\bullet +}$ [Reaction (2)].[7]

$$e_{aq}^- + S_2O_8^{2-} \rightarrow SO_4^{2-} + SO_4^{\bullet -} \quad (1)$$

$$SO_4^{\bullet -} + A \text{ (or } AH^+) \rightarrow SO_4^{2-} + A^{\bullet +} \text{ (or } AH^{\bullet 2+}) \quad (2)$$

$$A^{\bullet +} \text{(or } AH^{\bullet 2+}) \rightarrow A^\bullet \text{ (or } AH^{\bullet +}) + H^+ \quad (3)$$

The TA spectra measured shortly after pulse radiolysis are characterized by positive signals at around 450 nm, which correspond to the absorption band of $SO_4^{\bullet -}$ (Figure 2a,b). With increasing time, the absorption band at around 450 nm disappears concomitant with the appearance of a new absorption band at around 600 nm (Figure 2a,b). At both pH 2.3 and pH 7.0, the time constant of the rising component observed at 600 nm matches well with the fast decay observed at 460 nm (Figure 2c, d). This result indicates that $\mathbf{AH}^{\bullet 2+}$(N1 + H^+) or $\mathbf{A}^{\bullet +}$ is formed by charge transfer between $SO_4^{\bullet -}$ and $\mathbf{AH}^+$ or **A** [Reaction (2)]. From the global fit analysis, the rate constants for the rise component observed at 600 nm were determined to be 5.9×10^6 and 7.7×10^6 s^{-1} at pH 2.3 and 7.0, respectively. By using TA spectroscopy in combination with pulse radiolysis of a 5 mM **A** solution, Kobayashi reported that the pK_a of N6-H of $\mathbf{A}^{\bullet +}$ is 4.2.[7] Close[15] and Chen et al.[33] predicted the pK_a of $\mathbf{A}^{\bullet +}$ to be 3.9 and 3.2, respectively. In this regard, in practice it is difficult for deprotonation to occur at the N6-H position of $\mathbf{AH}^{\bullet 2+}$ at pH < 4, which is lower than the pK_a (4.2) of N6-H. Thus, the rate constant of 5.9×10^6 s^{-1} at pH 2.3 has been assigned to that for the oxidation of AH^+. Furthermore, Kobayashi reported that at pH 7.2, the rising component of the time profile monitored at 600 nm corresponds to the formation of $\mathbf{A}^\bullet$(N6-H) through the deprotonation of $\mathbf{A}^{\bullet +}$ [Reaction (3)], which occurs with a rate constant of 2.0×10^7 s^{-1}.[7] The rate constant of 2.0×10^7 s^{-1} reported by Kobayashi is 2.6-fold larger than that measured for 2 mM A at pH 7.0 in this study (7.7×10^6 s^{-1}). This difference can be interpreted by different rate-determining steps in solutions of low and high **A** concentration. Considering the pathway for the oxidation of **A**, the oxidation reaction [Reaction (2)], which is a bimolecular reaction, is the rate-determining step at low adenosine concentration, whereas the deprotonation process [Reaction (3)], which is a unimolecular reaction, is the rate-determining step at high **A** concentration because Reaction (2) will be faster. Kobayashi used a 5 mM adenosine concentration, which is higher than that used in this study (2 mM). Thus, the rising kinetics (2.0×10^7 s^{-1}) at 600 nm reported by Kobayashi for a 5 mM **A** concentration derives from the deprotonation process, which is the rate-determining step. However, in this study the rate constant of 7.7×10^6 s^{-1} determined at pH 7.0 cannot be assigned to the deprotonation process, because the rate constants determined at both pH 2.3 and 7.0 have similar values. In this case, if both the oxidation and the deprotonation processes occur with a similar rate constant, both processes would contribute to the observed kinetics. Therefore, we suggest that the kinetics determined from the rising component at neutral pH ($\geq$4.6) can be attributed to both the oxidation and deprotonation processes. From these points of view, we speculate that in a neutral pH ($\geq$5) solution, the radical cation $\mathbf{A}^{\bullet +}$ generated by one-electron oxidation undergoes deprotonation leading to the formation of $\mathbf{A}^\bullet$, whereas deprotonation at the N6-H position of $\mathbf{AH}^{\bullet 2+}$ in acidic pH solution (<4) is unlikely to occur because the pK_a of N6-H is 4.2. Therefore, we suggest that the absorption band observed at around 600 nm at pH 2.3 and 7.0 are attributed to $\mathbf{AH}^{\bullet 2+}$ and $\mathbf{A}^\bullet$, respectively.

To further elucidate the proton transfer occurring in $\mathbf{A}^{\bullet +}$, TA spectra were recorded 500 ns after pulse radiolysis of 2 mM $\mathbf{AH}^+$(N1 + H^+) and **A** in solutions at various pH. As shown in Figure 3 with increasing pH, the broad absorption band ob-

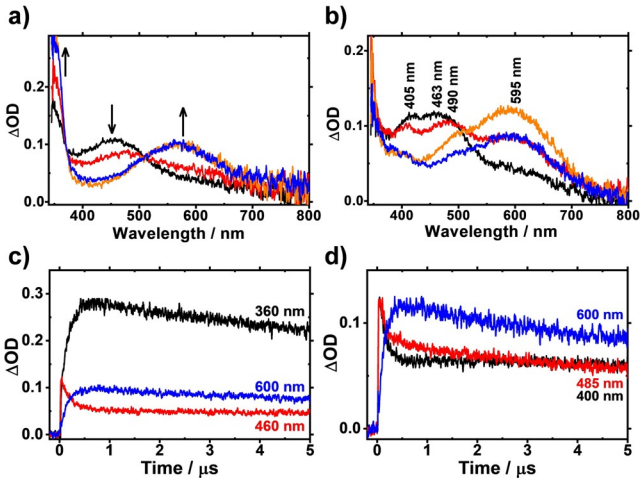

Figure 2. a) Transient absorption spectra observed at various times after 8 ns electron pulse radiolysis of 2 mM $\mathbf{AH}^+$ at pH 2.3. b) Transient absorption spectra observed at various times after 8 ns electron pulse radiolysis of 2 mM **A** at pH 7.0. The arrows in parts (a) and (b) indicate the direction of intensity changes with time at the two maxima. c) Decay profiles monitored at several wavelengths after 8 ns electron pulse radiolysis of 2 mM $\mathbf{AH}^+$ at pH 2.3. d) Decay profiles monitored at several wavelengths after 8 ns electron pulse radiolysis of 2 mM **A** at pH 7.0.

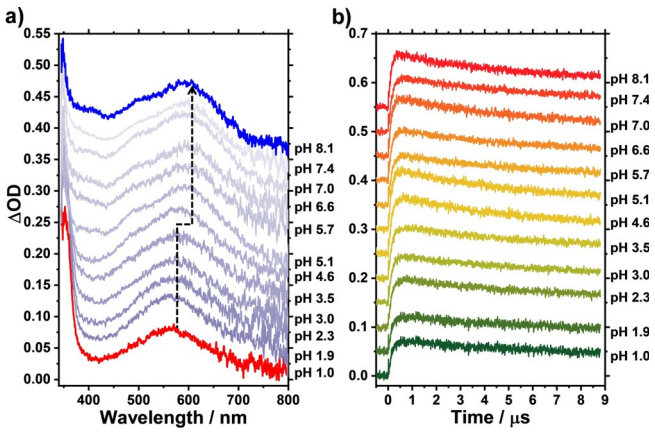

Figure 3. a) TA spectra recorded at 500 ns after 8 ns electron pulse radiolysis of 2 mM adenosine ($\mathbf{A}H^+$ and **A** depending on pH) solutions at various pH. b) Decay profiles of solutions at various pH monitored at 600 nm.

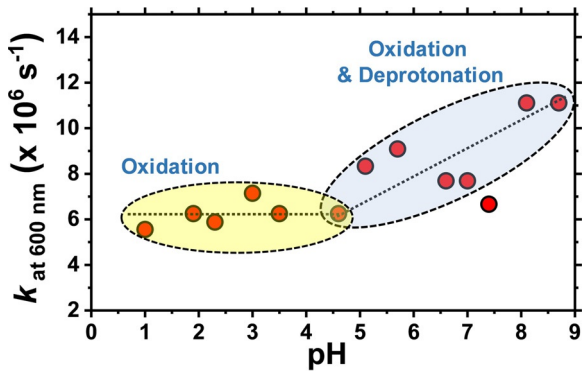

Figure 4. pH dependence of the rate constants (k_r) determined from the rise component of the time profiles monitored at 600 nm.

served at around 600 nm is slightly redshifted and new absorption bands at around 410 and 500 nm appear at pH > 4.6. These spectral changes indicate that the origin of the absorption band at around 600 nm changes at pH ≈ 4.6. Kobayashi[7] and Scheek et al.[34] reported pK_a values of 4.2 and 4 for $A^{\bullet+}$, respectively, whereas Steenken[35] reported a much lower value (≤ 1), which was supported by Sevilla and co-workers[17] through their EPR study and theoretical calculations. In contrast, Close[15] and Chen et al.[33] predicted the pK_a values of $\mathbf{A}^{\bullet+}$ to be 3.9 and 3,2, respectively. In particular, Close[15] suggested that the low pK_a value predicted by Sevilla and co-workers was due to an inappropriate calculation method and that the pK_a of $\mathbf{A}^{\bullet+}$ is not actually ≤ 1 but 3.9, which is close to the experimental value determined by Kobayashi.[7] We note that the pH value of approximately 4.6, at which the spectral change is observed, is close to the pK_a of $A^{\bullet+}$ reported by Kobayashi,[7] Close,[15] and Scheek et al.[34] Thus, we suggest that the pK_a of N6-H of $\mathbf{A}^{\bullet+}$ is about 4.6. In addition, a plot of the rate constants (k_r) for the rise component at 600 nm against pH shows that the k_r values at pH ≥ 4.6 increase with pH, whereas at pH ≤ 4.6, constant k_r values ($(6.2 \pm 0.5) \times 10^6\ s^{-1}$) are observed (Figure 4). As mentioned above, the kinetics determined from the rising component at neutral pH (≥ 4.6) have been attributed to both the oxidation and deprotonation processes. Generally, the deprotonation process is accelerated with increasing pH because of the decrease in proton concentration. Therefore, at pH ≥ 4.6, the increase in k_r with increasing pH is probably due to the acceleration of the deprotonation process. Meanwhile, the constant k_r values determined at acidic pH (≤ 4.6) are probably due to the absence of the deprotonation process in $\mathbf{A}H^{\bullet 2+}$; in practice it is difficult for deprotonation to occur at the N6-H position of $\mathbf{A}H^{\bullet 2+}$ at pH values lower than the pK_a (4.2) of N6-H. Thus, we conclude that the absorption band observed at around 600 nm at pH 2.3 and 7.0 can be attributed to $\mathbf{A}H^{\bullet 2+}$(N1 + H^+) and $\mathbf{A}^{\bullet}$, respectively.

Next, we considered the possibility of the formation of $\mathbf{AA}^{\bullet+}$ in high-concentration solutions. Sevilla and co-workers reported that the spectrum of $\mathbf{AA}^{\bullet+}$ in the visible region is similar to that of $\mathbf{A}^{\bullet+}$, and thus we cannot rule out the possibility of the formation of $\mathbf{AA}^{\bullet+}$ as well as $\mathbf{A}^{\bullet+}$.[17] In principle, $\mathbf{AA}^{\bullet+}$ can be formed by the direct oxidation of **AA** or by extremely fast association between **A** and $\mathbf{A}^{\bullet+}$. As mentioned above, however, **A** at neutral pH exists predominantly as the monomer even in high-concentration solutions. Thus, we can rule out the possibility of the formation of $\mathbf{AA}^{\bullet+}$ by the direct oxidation of **AA**. However, $\mathbf{AA}^{\bullet+}$ can be formed when the association between **A** and $\mathbf{A}^{\bullet+}$ is faster than the deprotonation of $\mathbf{A}^{\bullet+}$. Sevilla and co-workers reported that deprotonation of the charge-resonance-stabilized dimer $\mathbf{AA}^{\bullet+}$ is probably decelerated by the high pK_a of about 7.[17] At high concentrations, the oxidation process [Reaction (2)] would be faster. Furthermore, if $\mathbf{AA}^{\bullet+}$ were formed and its pK_a were around 7, then the rate of the deprotonation process of $\mathbf{AA}^{\bullet+}$ would be slower than that of $\mathbf{A}^{\bullet+}$, the pK_a of which is around 4. In this case, therefore, the rate-determining step would be the deprotonation process responsible for the rising kinetics observed at 600 nm. To investigate the possibility of this scenario, we measured the TA spectra at a much higher concentration (20 mM **A** at pH 7.0) than 2 mM and compared them with those obtained at low concentration (2 mM). As shown in Figure 5 a,b, no change in the spectrum due to an increase in the concentration of **A** was observed. These results indicate that there is no association between **A** and radical species such as $\mathbf{A}^{\bullet+}$ and $\mathbf{A}^{\bullet}$ that induces spectral change in the TA spectrum even in high-concentration solutions. Furthermore, as shown in Figure 5 c, the time profile recorded at a high concentration shows a relatively fast rising feature compared to that measured with a low concentration: The corresponding rate constants were determined to be 7.3×10^6 and $4.7 \times 10^7\ s^{-1}$ in 2 and 20 mM **A** solutions, respectively. The rate constant of $4.7 \times 10^7\ s^{-1}$ in the 20 mM solution is close to the rate constant for the deprotonation of monomer $\mathbf{A}^{\bullet+}$ reported by Kobayashi.[7] This result supports the idea that there is no association between **A** and $\mathbf{A}^{\bullet+}$ under our experimental conditions and that the absorption band observed at around 600 nm in the 20 mM **A** solution can be attributed to $\mathbf{A}^{\bullet}$(N6-H^+), not $\mathbf{AA}^{\bullet+}$.

To provide a detailed structural description of the species $\mathbf{A}H^{\bullet 2+}$ and $\mathbf{A}^{\bullet}$(N6−H) observed in acidic and neutral pH solutions, respectively, we measured the TR^3 spectra at 200 ns after pulse radiolysis of $\mathbf{A}H^+$ and **A** at pH 2.6 and 7.0, respectively,

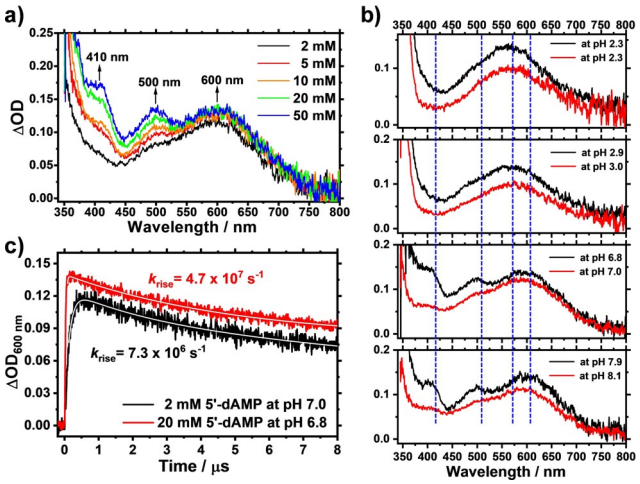

Figure 5. a) TA spectra recorded at 500 ns after an 8 ns electron pulse as a function of **A** concentration at pH 7.0. b) Comparison of the transient absorption spectra recorded at 500 ns after 8 ns electron pulse radiolysis of 2 (red) and 20 mM (black) **A** solutions at various pH. c) Time profiles monitored at 600 nm at pH 7.0. Theoretical fit curves are shown as white solid lines.

by using 532 nm laser pulses. Based on the results of our TA experiments, we suggest that the TR^3 spectra recorded 200 ns after pulse radiolysis of $\mathbf{A}H^+(N1+H^+)$ and **A** originate from $\mathbf{A}H^{\bullet 2+}(N1+H^+)$ and $\mathbf{A}^{\bullet}(N6-H)$, respectively. As shown in Figure 6, the TR^3 spectra of $\mathbf{A}H^{\bullet 2+}(N1+H^+)$ and $\mathbf{A}^{\bullet}(N6-H)$ recorded after 200 ns are very different to those of $\mathbf{A}H^+$ and **A**, which indicates that the structures of $\mathbf{A}H^{\bullet 2+}(N1+H^+)$ and $\mathbf{A}^{\bullet}(N6-H)$ are very different to those of $\mathbf{A}H^+$ and **A**, respectively. The TR^3 spectrum of $\mathbf{A}^{\bullet}(N6-H)$ shows intense bands centered at 1267, 1329, 1391, and 1445 cm^{-1}, whereas the spectrum of $\mathbf{A}H^{\bullet 2+}(N1+H^+)$ exhibits intense Raman bands centered at 1377, 1394, 1462, and 1546 cm^{-1}. To assign the Raman bands of $\mathbf{A}H^{\bullet 2+}(N1+H^+)$ and $\mathbf{A}^{\bullet}$(N6-H$^+$), we carried out DFT calculations to determine the minimum-energy structures, vibrational frequencies, and Raman activities of $\mathbf{A}H^{\bullet 2+}$ and $\mathbf{A}^{\bullet}(N6-H)$. As shown in Figure S3 in the Supporting Information, reasonable agreement between the experimental and theoretical Raman spectra of $\mathbf{A}H^{\bullet 2+}(N1+H^+)$ and $\mathbf{A}^{\bullet}(N6-H)$ was obtained, although a smaller scaling factor (0.93) was used to achieve a better agreement between the experimental and calculated Raman peaks of $\mathbf{A}H^{\bullet 2+}(N1+H^+)$. The up-shifted calculated vibration calculated vibration frequencies for $\mathbf{A}H^{\bullet 2+}(N1+H^+)$, obtained by using an implicit solvation model (CPCM), might be due to the delocalization of the 2+ charge of the adenine moiety into the whole adenosine molecule, which results in a reduction of the effective charge of the adenine moiety. The Raman bands of $\mathbf{A}H^{\bullet 2+}(N1+H^+)$ and $\mathbf{A}^{\bullet}(N6-H)$ in acidic and neutral pH solutions have been assigned on the basis of the calculated Raman spectra and are listed in Table 1. The Raman bands of $\mathbf{A}H^{\bullet 2+}(N1+H^+)$ centered at 1377, 1394, 1462, and 1546 cm^{-1} have been assigned to Im, Im, and Pyr ring stretching vibrations, and to the Pyr+NH$_2$ scissoring vibration, respectively. The observation of a Raman band at 1546 cm^{-1}, which corresponds to the Pyr+NH$_2$ scissoring vibration, supports the proposal that in acidic solutions the final product generated by the oxidation of adenosine is $\mathbf{A}H^{\bullet 2+}(N1+H^+)$, not $\mathbf{A}H^{\bullet +}(N1+H^+, N6-H)$. Compared with the Raman bands of $\mathbf{A}H^+$, the Raman bands of $\mathbf{A}H^{\bullet 2+}(N1+H^+)$ are significantly down-shifted, indicating a decrease in the bond order of the pyrimidine and imidazole rings due to the resonance structure of $\mathbf{A}H^{\bullet 2+}(N1+H^+)$. On the other hand, the Raman bands of $\mathbf{A}^{\bullet}(N6-H)$ centered at 1267, 1329, 1391, and 1445 cm^{-1} have been assigned to Pyr, Pyr+Im, Im, and Pyr+Im ring stretching vibrations, respectively, whereas the weak Raman bands at 1525 and 1572 cm^{-1} have been attributed to Im and Pyr ring stretching vibrations, respectively. Furthermore, in the case of $\mathbf{A}^{\bullet}(N6-H)$, we could not observe a Raman band corresponding to the Pyr+NH$_2$ scissoring vibration. This absence is due to the deprotonation at the N6 position upon oxidation. This result supports the idea that the TR^3 spectrum observed 200 ns after pulse radiolysis of **A** at pH 7 originates from $\mathbf{A}^{\bullet}(N6-H)$.

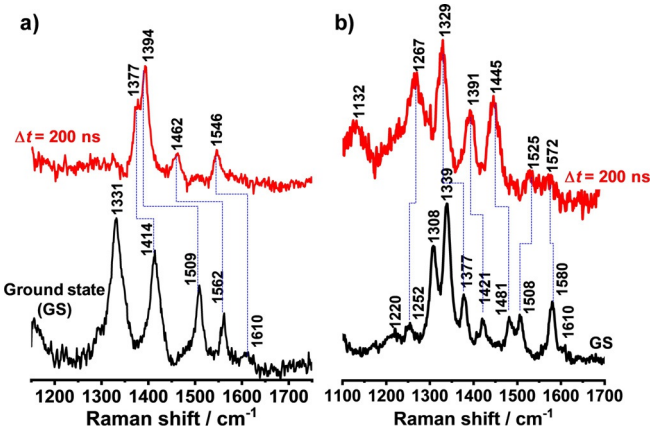

Figure 6. TR^3 spectra recorded at 200 ns after 8 ns electron pulse radiolysis of a) 20 mM $\mathbf{A}H^+$ at pH 2.3 and b) 20 mM **A** at pH 7.0 (λ_{ex} = 532 nm).

On the other hand, if the pK_a of N1 of $\mathbf{A}H^{\bullet 2+}(N1+H^+)$ formed by one-electron oxidation at acidic pH were very low, $\mathbf{A}^{\bullet +}(N1-H^+)$ could be formed as a final product by the release of the bound N1 proton (see Scheme 2a). To explore the possibility of the formation of $\mathbf{A}^{\bullet +}(N1-H^+)$ at acidic pH, we calculated its Raman spectrum and compared it with the TR^3 spectrum measured at pH 2.3. As shown in Figure S4 in the Supporting Information, the calculated Raman spectrum of $\mathbf{A}^{\bullet +}(N1-H^+)$ is significantly different to the TR^3 spectrum measured at pH 2.3, whereas the calculated Raman spectra of $\mathbf{A}H^{\bullet 2+}(N1+H^+)$ is similar. On the basis of this comparison between the calculated and recorded TR^3 spectra, we suggest that the TR^3 spectrum measured at pH 2.3 can be attributed to $\mathbf{A}H^{\bullet 2+}(N1+H^+)$ and that the pK_a of N1 of $\mathbf{A}H^{\bullet 2+}(N1+H^+)$ is higher than 2.3.

The results presented herein clearly show the oxidation of adenosine at acidic and neutral pH results in the formation of $\mathbf{A}H^{\bullet 2+}(N1+H^+)$ and $\mathbf{A}^{\bullet}(N6-H)$, respectively (see Scheme 2a). The fact that in acidic solution the final product generated by the oxidation of adenosine is $\mathbf{A}H^{\bullet 2+}(N1+H^+)$, not $\mathbf{A}^{\bullet +}(N1+H^+, N6-H)$, which is the deprotonated form of $\mathbf{A}H^{\bullet 2+}(N1+H^+)$, may have biological importance. According to previous studies, in neutral aqueous solution, $\mathbf{A}^{\bullet}(N6-H)$ can be protonated to $\mathbf{A}H^{\bullet +}(N1+H^+, N6-H)$, which can generate the C8-OH

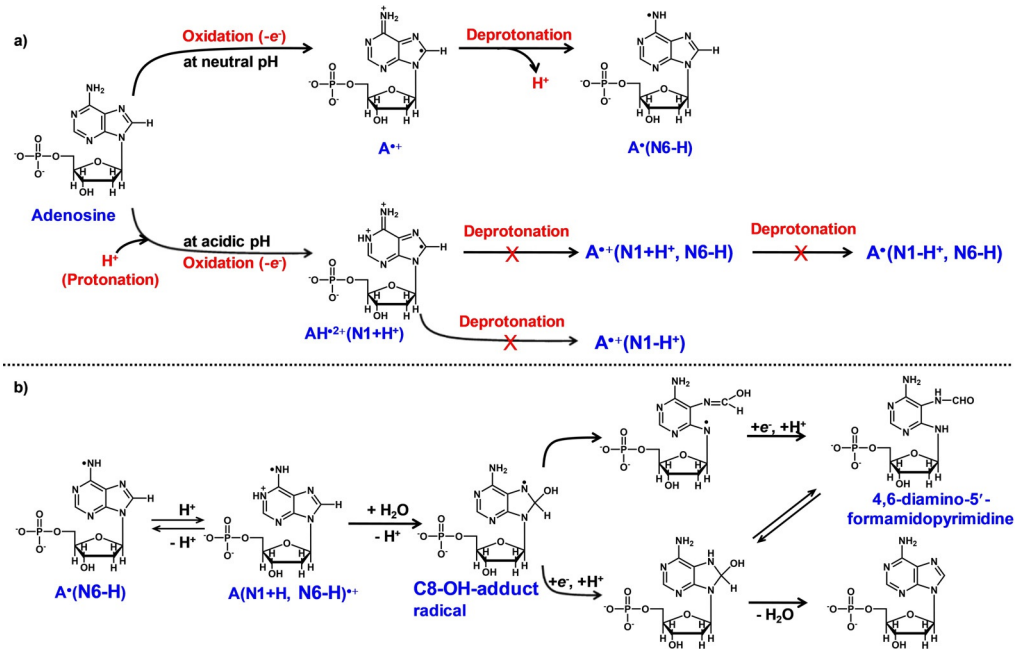

Scheme 2. a) Oxidation of adenosine in acidic and neutral pH solutions according to the results of this work. b) Reactions of **A**•(N6−H) with H^+ and e^- known to occur in biological systems.[38]

adduct radical upon hydration (see Scheme 2 b).[36–38] The C8-OH adduct radical can be converted into 4,6-diamino-5-formamidopyrimidine (see Scheme 2 b), which is a major lesion generated in DNA in in vitro and in vivo conditions by the ring-opening reaction of the imidazole ring and subsequent one-electron reduction.[36–38] Our results suggest that the formation of 4,6-diamino-5-formamidopyrimidine may be prevented in acidic solution in which the formation of **A**•(N6−H) and **A**H•+ (N1 + H+, N6−H) is inhibited.

Conclusions

In this study, TA and TR^3 spectroscopic methods in combination with pulse radiolysis were used to investigate in detail the oxidation of **A** in acidic and neutral solutions. The results presented herein demonstrate that **A** in acidic and neutral solutions exists in its protonated (**A**H+(N1 + H+)) and neutral (**A**) forms, respectively. The oxidation of **A** in neutral pH conditions induces the formation of **A**• because N6-H in **A**•+ has a pK_a of 4.2. In contrast, at acidic pH, **A**H•2+(N1 + H+), generated with a rate constant of $(6.2 \pm 0.5) \times 10^6\ s^{-1}$ by pulse radiolysis of **A**H+ (N1 + H+), does not undergo the deprotonation process because its pK_a is higher than the pH of the solution. In addition, the results presented here clearly demonstrate that **A**, **A**H+ (N1 + H+), and their radical species exist as monomers in the concentration range of 2–50 mM. On the other hand, based on the results of TA experiments, we can conclude that the TR^3 spectra observed at 200 ns after pulse radiolysis of **A**H+(N1 + H+) and **A** originate from **A**H•2+(N1 + H+) and **A**•, respectively. Compared with the Raman bands of **A**H+, the Raman bands of **A**H•2+(N1 + H+) appear at a significantly lower energy, which indicates a decrease in the bond order of the pyrimidine and imidazole rings due to the resonance structure of **A**H•2+(N1 + H+). The **A**•(N6−H) species does not show a Raman band corresponding to a Pyr + NH_2 scissoring vibration due to deprotonation at the N6 position upon oxidation. Our results may be relevant for studies of oxidative DNA damage initiated by the radical cations of nucleotides.

Experimental Section

General

2′-Deoxyadenosine-5′-monophosphate (5′-dAMP), that is, **A**, was purchased from Sigma–Aldrich and used without further purification. Ammonium persulfate ($(NH_4)_2S_2O_8$) and *tert*-butyl alcohol were purchased from Wako Pure Chemical Industries Ltd. and Nacalai Tesque, respectively, and used without purification. Aqueous solutions of 5′-dAMP containing 0.1 M $(NH_4)_2S_2O_8$, 100 mM sodium phosphate buffer, and 0.1 M *tert*-butyl alcohol (for the scavenging of OH• radicals) were saturated with argon gas by bubbling for 15 min at room temperature before radiolysis.

TA spectroscopy with pulse radiolysis

The experimental setup used for pulse radiolysis was similar to that reported previously.[19] Briefly, pulse radiolysis experiments on **A** were performed with an 8 ns electron pulse (27 MeV, 11 A, 8 ns, 0.8 kGy per pulse) generated by a linear accelerator at Osaka University. The probe light was obtained from a pulsed 450 W xenon arc lamp (Ushio, UXL-451-0). The kinetic measurements were performed by using a nanosecond photoreaction analyzer system (Unisoku, TSP-1000). The probe beam passing through the sample was focused on the entrance slit of a monochromator (Unisoku, MD200) and detected with a photomultiplier tube (Hamamatsu Photonics, R2949). The TA spectra were measured by using a photodiode array (Hamamatsu Photonics, S3904-1024F) with a gated image intensifier (Hamamatsu Photonics, C2925-01) as a detector.

TR^3 spectroscopy with pulse radiolysis

The TR^3 experimental setup for pulse radiolysis was similar to that reported previously.[13,21] The TR^3 spectra of adenosine after exposure to an 8 ns electron pulse were obtained by excitation with a 532 nm flash, which was the second harmonic of a nanosecond Q-switched Nd:YAG laser (5 ns full-width at half-maximum (FWHM), Brilliant, Quantel; Les Ulis, France). The laser excitation light was synchronized with an 8 ns electron pulse. The TR^3 spectra were collected by using a monochromator (Acton, SP2500i, Trenton, NJ, USA) equipped with a charge-coupled device (CCD) camera (Princeton Instruments, PI-MAX3, Trenton, NJ, USA).

DFT calculations

The Raman spectra of neutral and protonated adenosine were calculated by DFT methods at the B3LYP-D3/6-311++G(d,p) level of theory by using the conductor-like polarizable continuum model (CPCM), which includes water solvation effects. All the geometries used for simulation were optimized prior to calculation of the Raman activities. For radical species generated by pulse radiolysis, unrestricted B3LYP (UB3LYP), with the same basis set, was used. The charge state for the phosphate group was set to -1 ($P(OH)O_2^-$). The calculated Raman peaks were scaled by 0.982 or 0.93, and convoluted by using a Gaussian function (FWHM = 8 cm^{-1}). All geometry optimizations and Raman activity calculations were performed by using the Gaussian 16 package.[39]

Acknowledgements

We would like to thank the members of the Research Laboratory for Quantum Beam Science of ISIR, Osaka University, for running the linear accelerator. This work was partly supported by a Grant-in-Aid for Scientific Research from the Ministry of Education, Culture, Sports, Science and Technology (MEXT) of the Japanese Government (Projects 25220806 and 25288035), and by the Institute for Basic Science (IBS-R004).

Conflict of interest

The authors declare no conflict of interest.

Keywords: nucleotides · oxidation · proton transfer · pulse radiolysis · Raman spectroscopy

[1] S. Steenken, J. P. Telo, H. M. Novais, L. P. Candeias, *J. Am. Chem. Soc.* **1992**, *114*, 4701 – 4709.
[2] I. Saito, M. Takayama, H. Sugiyama, K. Nakatani, *J. Am. Chem. Soc.* **1995**, *117*, 6406 – 6407.
[3] H. Sugiyama, I. Saito, *J. Am. Chem. Soc.* **1996**, *118*, 7063 – 7068.
[4] F. Prat, K. N. Houk, C. S. Foote, *Abstr. Pap. Am. Chem. Soc.* **1998**, *216*, U456.
[5] Y. Yoshioka, Y. Kitagawa, Y. Takano, K. Yamaguchi, T. Nakamura, I. Saito, *J. Am. Chem. Soc.* **1999**, *121*, 8712 – 8719.
[6] A. Kumar, M. D. Sevilla, *J. Phys. Chem. B* **2009**, *113*, 11359 – 11361.
[7] K. Kobayashi, *J. Phys. Chem. B* **2010**, *114*, 5600 – 5604.
[8] L. Wu, K. Liu, J. Jie, D. Song, H. Su, *J. Am. Chem. Soc.* **2015**, *137*, 259 – 266.
[9] K. Kobayashi, S. Tagawa, *J. Am. Chem. Soc.* **2003**, *125*, 10213 – 10218.
[10] S. Steenken, *Chem. Rev.* **1989**, *89*, 503 – 520.
[11] T. Ito, S. Kuno, T. Uchida, S.-i. Fujita, S.-i. Nishimoto, *J. Phys. Chem. B* **2009**, *113*, 389 – 394.
[12] K. Kobayashi, R. Yamagami, S. Tagawa, *J. Phys. Chem. B* **2008**, *112*, 10752 – 10757.
[13] J. Choi, C. Yang, M. Fujitsuka, S. Tojo, H. Ihee, T. Majima, *J. Phys. Chem. Lett.* **2015**, *6*, 5045 – 5050.
[14] O. B. Morozova, N. N. Fishman, A. V. Yurkovskaya, *Phys. Chem. Chem. Phys.* **2017**, *19*, 21262 – 21266.
[15] D. M. Close, *J. Phys. Chem. A* **2013**, *117*, 473 – 480.
[16] V. Verdolino, R. Cammi, B. H. Munk, H. B. Schlegel, *J. Phys. Chem. B* **2008**, *112*, 16860 – 16873.
[17] A. Adhikary, A. Kumar, D. Khanduri, M. D. Sevilla, *J. Am. Chem. Soc.* **2008**, *130*, 10282 – 10292.
[18] M. Fujitsuka, T. Majima, *J. Phys. Chem. Lett.* **2011**, *2*, 2965 – 2971.
[19] J. Choi, M. Fujitsuka, S. Tojo, T. Majima, *J. Am. Chem. Soc.* **2012**, *134*, 13430 – 13435.
[20] N. M. Dimitrijevic, D. M. Bartels, C. D. Jonah, K. Takahashi, T. Rajh, *J. Phys. Chem. B* **2001**, *105*, 954 – 959.
[21] J. Choi, D. W. Cho, S. Tojo, M. Fujitsuka, T. Majima, *J. Phys. Chem. A* **2015**, *119*, 851 – 856.
[22] J. Choi, D. W. Cho, S. Tojo, M. Fujitsuka, T. Majima, *Mol. BioSyst.* **2015**, *11*, 218 – 222.
[23] F. Tureček, X. H. Chen, *J. Am. Soc. Mass Spectrom.* **2005**, *16*, 1713 – 1726.
[24] R. C. Lord, G. J. Thomas, *Spectrochim. Acta Part A* **1967**, *23*, 2551 – 2591.
[25] L. E. Bailey, R. Navarro, A. Hernanz, *Biospectroscopy* **1997**, *3*, 47 – 59.
[26] S. P. A. Fodor, T. G. Spiro, *J. Am. Chem. Soc.* **1986**, *108*, 3198 – 3205.
[27] N. Fujimoto, A. Toyama, H. Takeuchi, *J. Mol. Struct.* **1998**, *447*, 61 – 69.
[28] A. Toyama, Y. Takino, H. Takeuchi, I. Harada, *J. Am. Chem. Soc.* **1993**, *115*, 11092 – 11098.
[29] K. J. Neurohr, H. H. Mantsch, *Can. J. Chem.* **1979**, *57*, 1986 – 1994.
[30] L. P. Candeias, S. Steenken, *J. Am. Chem. Soc.* **1989**, *111*, 1094 – 1099.
[31] L. P. Candeias, S. Steenken, *J. Am. Chem. Soc.* **1993**, *115*, 2437 – 2440.
[32] P. O. P. Ts'o, J. Eisinger, *Basic Principles in Nucleic Acid Chemistry*, Academic Press, New York, **1974**.
[33] X. Chen, E. A. Syrstad, M. T. Nguyen, P. Gerbaux, F. Tureček, *J. Phys. Chem. A* **2004**, *108*, 9283 – 9293.
[34] R. M. Scheek, S. Stob, T. Schleich, N. C. M. Alma, C. W. Hilbers, R. Kaptein, *J. Am. Chem. Soc.* **1981**, *103*, 5930 – 5932.
[35] S. Steenken, *Free Radical Res. Commun.* **1992**, *16*, 349 – 379.
[36] C. Chatgilialoglu, P. O'Neill, *Exp. Gerontol.* **2001**, *36*, 1459 – 1471.
[37] M. Dizdaroglu, G. Kirkali, P. Jaruga, *Free Radical Biol. Med.* **2008**, *45*, 1610 – 1621.
[38] M. Dizdaroglu, P. Jaruga, *Free Radical Res.* **2012**, *46*, 382 – 419.
[39] M. J. Frisch, G. W. Trucks, H. B. Schlegel, G. E. Scuseria, M. A. Robb, J. R. Cheeseman, G. Scalmani, V. Barone, G. A. Petersson, H. Nakatsuji, X. Li, M. Caricato, A. V. Marenich, J. Bloino, B. G. Janesko, R. Gomperts, B. Mennucci, H. P. Hratchian, J. V. Ortiz, A. F. Izmaylov, J. L. Sonnenberg, Williams, F. Ding, F. Lipparini, F. Egidi, J. Goings, B. Peng, A. Petrone, T. Henderson, D. Ranasinghe, V. G. Zakrzewski, J. Gao, N. Rega, G. Zheng, W. Liang, M. Hada, M. Ehara, K. Toyota, R. Fukuda, J. Hasegawa, M. Ishida, T. Nakajima, Y. Honda, O. Kitao, H. Nakai, T. Vreven, K. Throssell, J. A. Montgomery, Jr., J. E. Peralta, F. Ogliaro, M. J. Bearpark, J. J. Heyd, E. N. Brothers, K. N. Kudin, V. N. Staroverov, T. A. Keith, R. Kobayashi, J. Normand, K. Raghavachari, A. P. Rendell, J. C. Burant, S. S. Iyengar, J. Tomasi, M. Cossi, J. M. Millam, M. Klene, C. Adamo, R. Cammi, J. W. Ochterski, R. L. Martin, K. Morokuma, O. Farkas, J. B. Foresman, D. J. Fox in *Gaussian 16 Rev. B.01*, *Vol.* Wallingford, CT, **2016**.

Manuscript received: February 15, 2019
Revised manuscript received: April 3, 2019
Accepted manuscript online: April 7, 2019
Version of record online: May 13, 2019